Far-infrared laser vibration–rotation–tunneling spectroscopy of water clusters in the librational band region of liquid water

Frank N. Keutsch
Department of Chemistry, University of California Berkeley, Berkeley, California 94720

Ray S. Fellers
Yahoo, 3420 Central Expressway, Santa Clara, California 95051

Mark R. Viant
Department of Animal Sciences, University of California, Davis, California 95616

Richard J. Saykally[a)]
Department of Chemistry, University of California Berkeley, Berkeley, California 94720

(Received 7 July 2000; accepted 10 November 2000)

We report the first high resolution spectrum of a librational vibration for a water cluster. Four parallel bands of $(H_2O)_3$ were measured between 510 and 525 cm^{-1} using diode laser vibration–rotation–tunneling (VRT) spectroscopy. The bands lie in the ''librational band'' region of liquid water and are assigned to the nondegenerate out of plane librational vibration. The observation of at least three distinct bands within 8 cm^{-1} originating in the vibrational ground state is explained by a dramatically increased splitting of the rovibrational levels relative to the ground state by bifurcation tunneling and is indicative of a greatly reduced barrier height in the excited state. This tunneling motion is of special significance, as it is the lowest energy pathway for breaking and reforming of hydrogen bonds, a salient aspect of liquid water dynamics. © *2001 American Institute of Physics.* [DOI: 10.1063/1.1337052]

I. INTRODUCTION

Small water clusters are of current experimental and theoretical interest for reasons discussed in many recent papers.[1–16] An extensive set of high precision vibration–rotation–tunneling (VRT) spectroscopy results now exists for small water clusters;[7,9,11,12,14,17–20] this has afforded a rigorous test of various water potentials and *ab initio* calculations, and has characterized the nature of the associated hydrogen bond tunneling dynamics. One of the exciting goals of this work is the determination of an accurate intermolecular potential for bulk phases of water. Following our comprehensive study of the dimer, a similar study of the water trimer is the next logical step as it allows explicit quantification of three-body forces which have not been included in the recently determined water pair potential.[10,21] Previous spectroscopic studies have been primarily limited to frequencies below ~3 THz (~100 cm^{-1}) and address torsional motions of the free hydrogen atoms, which are not thought to be a prominent feature of bulk water dynamics. Clearly, it would be interesting to investigate both vibrations which more closely resemble those observed in the bulk as well as higher energies of the intermolecular potential energy surface (IPS) corresponding to thermally activated bulk processes. The first results for the hydrogen bond stretching vibration of a water cluster, corresponding to the ''translational band'' of the liquid, are presented in the accompanying paper.[16]

The most prominent intermolecular vibrational band of liquid water is the ''librational band,'' extending from ~300–1000 cm^{-1} in H_2O. The hindered rotational motion of water molecules giving rise to this absorption feature is proposed to be of singular importance for the solvation and relaxation dynamics of the bulk phases.[22,23] Many different experimental methods, including neutron scattering, dielectric relaxation, Raman and IR spectroscopy have addressed these motions but there exists little consensus regarding the molecular details. No detailed experimental study that allows direct characterization of these librational motions on a microscopic level exists, and simulations which provide such a picture suffer from inaccuracy of bulk potentials.[24–31] The particular importance of the librations is that in each of the above processes the initial step in breaking of hydrogen bonds results from these rotational motions, whereas excitation of translational motions does not itself significantly facilitate breaking of hydrogen bonds.[32–34]

The free hydrogens in small water clusters—the main distinction of water clusters from the bulk—are predicted not to influence the librational motions to a large degree, and recent low resolution librational band spectra for water clusters containing 10–100 molecules do resemble bulk spectra.[35] Furthermore, computer simulations by Luzar and Chandler indicate that the hydrogen bond dynamics in liquid water are fairly insensitive to both the local hydrogen bond order and the effect of chemical environment, citing the example of a dimethylsulfoxide (DMSO) water system.[32–34] The fact that librational motions are thus very local and insensitive to the specific environment allows small water clusters to serve as models for elucidating the librational dynam-

[a)]Author to whom correspondence should be addressed. Electronic mail: saykally@uclink4.berkeley.edu

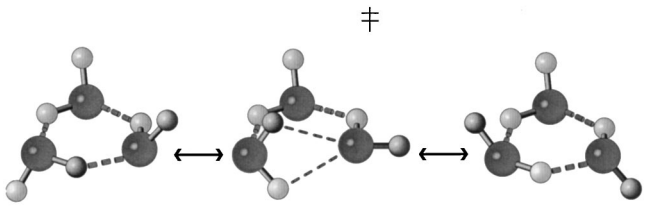

FIG. 1. The equilibrium structure of the water trimer, together with one of the two experimentally observed tunneling motions are shown. The bifurcation tunneling motion consists of the exchange of a free and a bound hydrogen atom together with the torsional flipping of a neighboring free hydrogen. It connects eight degenerate minima on the IPS and is the lowest energy hydrogen bond breaking motion observed in water clusters.

ics of liquid. Two types of librational modes are expected for cyclic water clusters: out-of-plane (OOP) and in-plane (IP) motions. The nuclear displacements of the OOP librational motion of a single water molecule closely resemble part of the bifurcation tunneling pathway, depicted in Fig. 1, which additionally includes the torsional (flipping) motion of a single free hydrogen on an adjacent water molecule. This bifurcation tunneling pathway is the lowest energy process for breaking and reforming hydrogen bonds in water clusters and is therefore of special interest.

We have investigated the frequency range from 515–528 cm^{-1} by diode laser VRT spectroscopy, thereby performing the first high-resolution measurements of water clusters in the ''librational band'' region of liquid water. Figure 2 shows a stick spectrum of the observed transitions for H_2O in relation to the ''librational band'' of the liquid. Altogether ~800 transitions have been measured, of which 135, generally the most intense, are assigned to the A_1^- OOP librational vibration of $(H_2O)_3$.

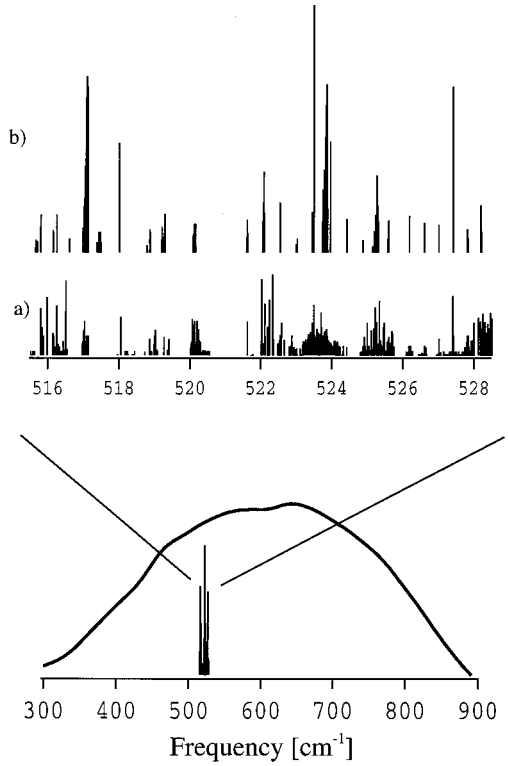

FIG. 2. An overview of the observed H_2O transitions with respect to the librational band of liquid H_2O shows that they are close to the center of the librational band of the liquid. Inset (a) shows the unassigned transitions and inset (b) shows the transitions assigned to $(H_2O)_3$ on the same relative intensity scale. The $(H_2O)_3$ transitions generally correspond to the most intense transitions.

II. EXPERIMENT

The Berkeley supersonic beam/diode laser spectrometer used in the observation of the new $(H_2O)_3$ bands has been described in detail previously and resembles the configuration used for our study of jet cooled uracil in the gas phase. Only the principal features and differences from the previously reported experimental setup will be presented here.[36,37]

A helium-cooled diode laser spectrometer (Spectra-Physics) using lead–salt diodes (Laser Photonics) was used to produce infrared radiation from 515–528 cm^{-1}. The infrared laser beam is multipassed 18–22 times through a pulsed planar supersonic expansion of a mixture of helium and H_2O using a Herriott cell configuration and detected by a liquid helium cooled (Si:B) photoconductive detector (Infrared Labs). The pulsed molecular beam is produced by expanding pure He, bubbled through liquid H_2O, through a 101.6 mm-long slit at a repetition rate of 35 Hz, while maintaining the vacuum chamber at approximately 200 mTorr by a Roots blower (Edwards EH4200) backed by two rotary pumps (Edwards E2M275). Simultaneously, the fringe spacing of a vacuum spaced étalon and an OCS reference gas spectrum are detected on a liquid helium cooled (Cu:Ge) detector (Santa Barbara Research Center) and recorded to enable precise frequency calibration of the water cluster scans. The observed linewidth of 30–40 MHz full width at half maximum (FWHM) is slightly larger than the Doppler limited linewidths extrapolated from our 140 cm^{-1} results. The typically obtainable frequency accuracy was 10–20 MHz, limited by the linewidths, drift of the diode laser, and accuracy of the frequency calibration.

The frequency range from 100–1200 cm^{-1} has been notoriously hard to access via high-resolution spectroscopic studies for a variety of reasons, most importantly the lack of a convenient laser system. The study reported here required the use of ten different diodes, each operating on several modes to cover the frequency range from 515–528 cm^{-1}. Even so, complete coverage of the region was not possible and several spectral gaps remain. Investigation of some regions was hindered by very strong atmospheric water absorptions, and the frequency accuracy of other regions is inferior due to a lack of suitable reference gas transitions and large frequency drift of some diode laser modes. Figure 2 shows an overview of the spectra measured in the 515–528 cm^{-1} range for pure H_2O clusters.

III. RESULTS

Four bands of $(H_2O)_3$ were measured between 515 and 528 cm^{-1}, representing the highest frequency water cluster intermolecular vibrational spectra observed to date. The identity of the spectral carrier was unambiguously established both through isotopic substitution studies, and through the fitted rotational constants. The transitions were assigned

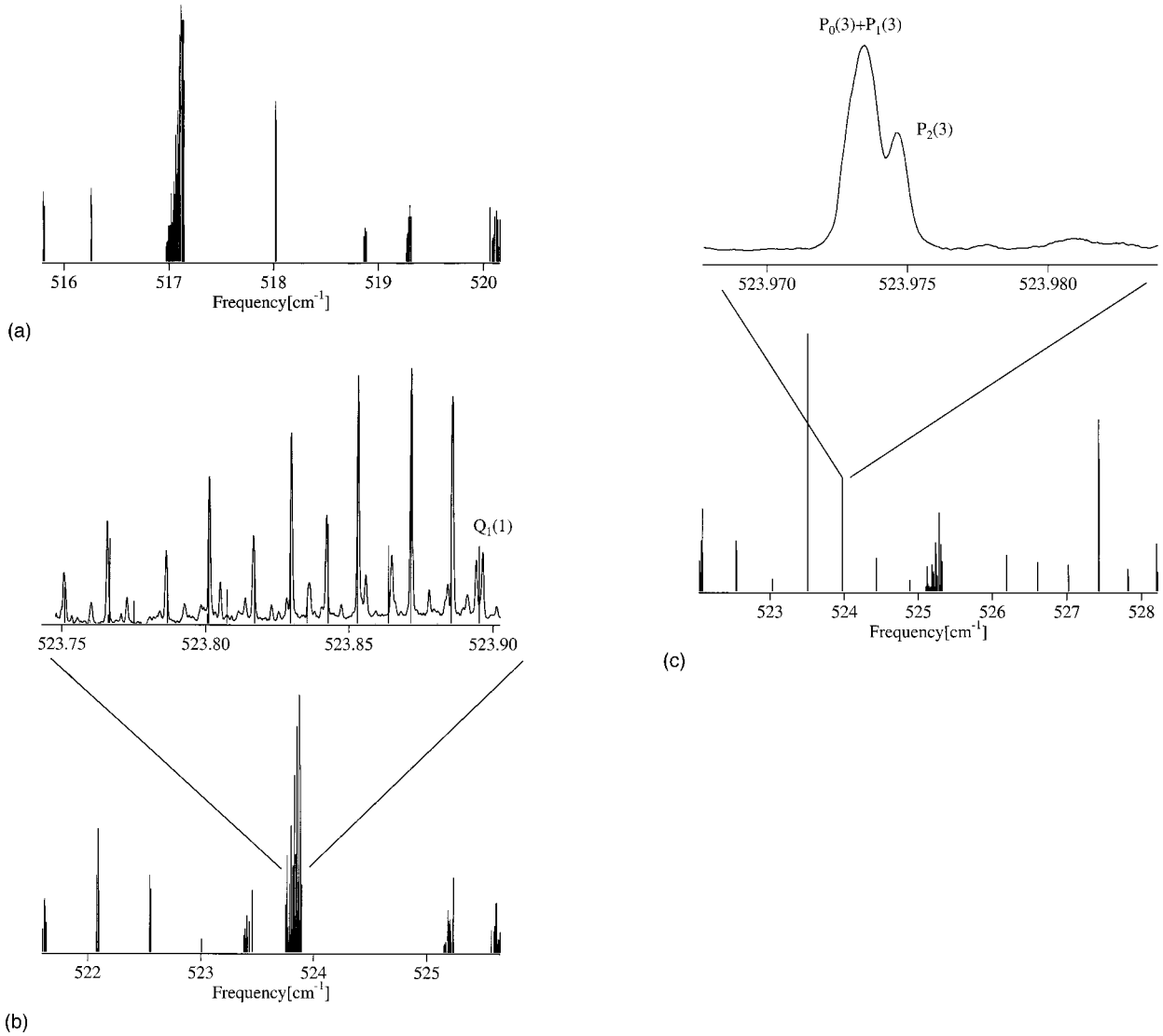

FIG. 3. (a) Spectral gaps only allowed the observation of the $P(2)$, $P(3)$, $R(1)$, $R(3)$, $R(4)$, and $R(6)$ branches of the 517.2 cm^{-1} band. The spectrum is typical for a parallel band of an oblate symmetric top. (b) A stick spectrum representation of the 523.9 cm^{-1} band is shown. The inset shows real data from the Q-branch region together with a stick spectrum representation of a simulation based on an oblate symmetric top energy expression and the molecular constants obtained from the fit. The rotational temperature in the simulation was 4 K. Comparison shows the $Q_1(1)$ transitions to be split into an equally spaced equal intensity doublet. (c) The 525.3 cm^{-1} band has the largest observed number of P- and R-branch transitions. The Q-branch region was scanned with a mode of inferior quality. The inset shows real data from the $P(3)$ transition and demonstrates that the $K=0$ and $K=1$ transitions could not be resolved separately.

either by identifying the Q-branch transitions and then using known vibrational ground state combination differences of $(H_2O)_3$ to assign P- and R-branch lines, or by directly using combination differences for the P- and R-branches. Analysis of the spectra was hindered by the lower absolute precision of the diode laser spectrometer as compared to the THz spectrometer[16] (however, the relative frequency accuracy is comparable at 1 ppm) and large gaps in the spectra, as described previously. A stick spectrum of the three assigned c-type bands together with the observed Q-branch of the 523.9 cm^{-1} band and $P(3)$ clump of the 525.3 cm^{-1} band is shown in Figs. 3(a)–3(c). These are typical for parallel bands of an oblate symmetric top. The most intense transitions were observed in the Q-branches and have a signal-to-noise ratio of about 200:1, compared to about 8000:1 for the most intense vibrations observed in THz spectroscopy experiments,[11] which arise from fairly intense torsional vibrations. The sensitivity of the diode laser experiment (10–100 ppm) is about two orders-of-magnitudes lower than that of the THz experiments, which indicates that these are indeed intense transitions, with the strongest being ~1% absorbers.

A. Analysis

The VRT bands were fit to the standard energy expression for an oblate symmetric top, $E=\nu+BJ(J+1)+(C-B)K^2-D_J[J(J+1)]^2-D_{JK}J(J+1)K^2-D_KK^4$. The fit of the 525.3 cm^{-1} band included an additional term $\pm\gamma J(J+1)$ to take the observed splitting of the $K=1$ lines into account. The assigned transition frequencies are shown in Table I(A)–(C) together with the difference between observed and calculated frequencies, and the molecular con-

TABLE I. The assigned transitions together with the difference between calculated and observed frequencies are shown. The excited states of the 517.2, 523.9, and 525.3 cm^{-1} bands are labeled as $\nu'=1$, 2, and 3, respectively. The high and low frequency component of the $K=1$ levels of the 523.9 cm^{-1} band are labeled 1 and 2, respectively. All values are in MHz.

(A)

517.2 cm^{-1} band	ν'	J'	K'	ν''	J''	K''	Frequency	Observed–calculated
	1	1	1	0	1	1	15 503 714.4	9.32
	1	2	2	0	2	2	15 503 535.9	1.75
	1	3	3	0	3	3	15 503 305.1	4.22
	1	3	2	0	3	2	15 503 043.9	4.74
	1	4	4	0	4	4	15 502 997.7	−6.99
	1	5	5	0	5	5	15 502 642.8	−2.89
	1	4	3	0	4	3	15 502 617.1	−5.32
	1	4	2	0	4	2	15 502 355.8	4.79
	1	6	6	0	6	6	15 502 232.5	8.16
	1	5	4	0	5	4	15 502 107.4	−21.17
	1	7	7	0	7	7	15 501 754	12.4
	1	6	5	0	6	5	15 501 550.2	−4.11
	1	8	8	0	8	8	15 501 200.5	1.71
	1	7	6	0	7	6	15 500 914.8	17.61
	1	9	9	0	9	9	15 500 604	6.23
	1	10	10	0	10	10	15 499 948.1	7.38
	1	11	11	0	11	11	15 499 222.2	−8.41
	1	1	1	0	2	1	15 477 118.9	0.35
	1	2	2	0	3	2	15 463 662.7	7.02
	1	2	1	0	3	1	15 463 510.5	5.65
	1	2	1	0	1	1	15 529 953.4	−15.3
	1	4	3	0	3	3	15 555 797.1	5.47
	1	4	2	0	3	2	15 555 529.5	11.84
	1	4	1	0	3	1	15 555 342.8	−11.18
	1	5	4	0	4	4	15 568 555.4	−31.45
	1	5	3	0	4	3	15 568 170.9	−12.33
	1	5	2	0	4	2	15 567 924.1	27.54
	1	5	1	0	4	1	15 567 731.6	6.38
	1	7	6	0	6	6	15 593 895.5	−32.97
	1	7	5	0	6	5	15 593 223.1	11.68
	1	7	3	0	6	3	15 592 175.7	−4.44
	1	7	2	0	6	2	15 591 873.6	12.91
	1	7	1	0	6	1	15 591 659	−10.59

(B)

523.9 cm^{-1} band	ν'	J'	K'	Label	ν''	J''	K''	Frequency	Observed–calculated
	2	1	1	1	0	1	1	15 706 006.4	−10.95
	2	1	1	2	0	1	1	15 705 940.5	−9.56
	2	2	2	0	0	2	2	15 705 694.2	2.64
	2	2	1	1	0	2	1	15 705 643.4	−7.55
	2	2	1	2	0	2	1	15 705 448.7	−0.23
	2	3	3	0	0	3	3	15 705 261.3	−11.09
	2	3	2	0	0	3	2	15 705 062	19.1
	2	4	4	0	0	4	4	15 704 717.9	−0.69
	2	4	3	0	0	4	3	15 704 390.9	−19.01
	2	4	2	0	0	4	2	15 704 214.2	23.22
	2	5	5	0	0	5	5	15 704 029.1	9.34
	2	5	4	0	0	5	4	15 703 638.1	−4.65
	2	6	6	0	0	6	6	15 703 177.1	14.63
	2	6	5	0	0	6	5	15 702 728.4	−2.34
	2	7	7	0	0	7	7	15 702 118.1	−12.33
	2	7	6	0	0	7	6	15 701 668.2	8.12
	2	4	4	0	0	5	4	15 638 261.8	1.48
	2	4	3	0	0	5	3	15 637 931.6	−24.4
	2	4	2	0	0	5	2	15 637 754.5	14.26
	2	4	1	2	0	5	1	15 637 256.7	−18.61
	2	4	1	1	0	5	1	15 637 931.6	−16
	2	3	3	0	0	4	3	15 652 090.3	−12.99
	2	3	2	0	0	4	2	15 651 904	27.72
	2	3	1	1	0	4	1	15 651 943.4	0.91

TABLE I. (*Continued.*)

(B) 523.9 cm^{-1} band	ν'	J'	K'	Label	ν''	J''	K''	Frequency	Observed–calculated
	2	3	1	2	0	4	1	15 651 547.4	8.28
	2	4	3	0	0	3	3	15 757 562.1	−16.9
	2	4	2	0	0	3	2	15 757 372.5	14.93
	2	4	1	1	0	3	1	15 757 562.1	0.57
	2	4	1	2	0	3	1	15 756 885.4	−3.83
	2	2	2	0	0	3	2	15 665 830.4	17.29
	2	2	1	1	0	3	1	15 665 777.6	4.28
	2	2	1	2	0	3	1	15 665 577.3	5.68
	2	1	1	1	0	2	1	15 679 432.6	1.87
	2	1	1	2	0	2	1	15 679 363.8	0.27
	2	0	0	0	0	1	0	15 692 856.2	−3.44

(C) 525.3 cm^{-1} band	ν'	J'	K'	ν''	J''	K''	Frequency	Observed–calculated
	3	0	0	0	1	0	15 735 684.5	−7.98
	3	1	1	0	1	1	15 748 752.9	−0.85
	3	1	1	0	2	1	15 722 174.1	6.85
	3	1	0	0	2	0	15 722 164.1	7.67
	3	2	2	0	2	2	15 748 295.3	−4.84
	3	2	2	0	3	2	15 708 407.1	−14.52
	3	2	1	0	2	1	15 748 263	−2.98
	3	2	1	0	3	1	15 708 380.7	−7.93
	3	2	0	0	3	0	15 708 370.7	−7.04
	3	2	1	0	1	1	15 774 851.4	−1.09
	3	2	0	0	1	0	15 774 841.4	0.42
	3	3	3	0	3	3	15 747 620.1	−5.89
	3	3	2	0	3	2	15 747 572.1	5.58
	3	3	2	0	4	2	15 694 411.2	11.27
	3	3	2	0	2	2	15 787 448.9	3.83
	3	3	1	0	3	1	15 747 527.6	−4.01
	3	3	1	0	4	1	15 694 362.3	−4.13
	3	3	0	0	4	0	15 694 352.3	−3.07
	3	3	1	0	2	1	15 787 409.7	0.83
	3	3	0	0	2	0	15 787 399.7	2.76
	3	4	3	0	4	3	15 746 641.3	−3.47
	3	4	3	0	5	3	15 680 196	5.14
	3	4	3	0	3	3	15 799 801.3	−12.6
	3	4	2	0	4	2	15 746 605.8	22.34
	3	4	2	0	5	2	15 680 147.2	14.55
	3	4	2	0	3	2	15 799 766	16
	3	4	1	0	4	1	15 746 551.1	3.87
	3	4	1	0	5	1	15 680 093.9	−4.47
	3	4	0	0	5	0	15 680 083.9	−3.15
	3	4	1	0	3	1	15 799 713.2	0.81
	3	4	0	0	3	0	15 799 703.2	3.25
	3	5	3	0	5	3	15 745 404.7	−5.36
	3	5	2	0	5	2	15 745 333.5	−12.8
	3	5	1	0	5	1	15 745 293.7	−15.07
	3	5	4	0	6	4	15 665 777.6	14.95
	3	5	4	0	4	4	15 811 936.9	−23.03
	3	5	3	0	4	3	15 811 876	11.97
	3	5	2	0	4	2	15 811 817.7	20.62
	3	5	2	0	6	2	15 665 648.8	32.34
	3	5	1	0	4	1	15 811 765.8	8.19
	3	5	0	0	4	0	15 811 755.8	11.24
	3	5	1	0	6	1	15 665 582.3	1.2
	3	5	0	0	6	0	15 665 572.3	2.88
	3	6	5	0	6	5	15 744 144.3	5.39
	3	6	1	0	6	1	15 743 795.6	−14.9
	3	6	5	0	5	5	15 823 884.5	−0.17
	3	6	4	0	5	4	15 823 740.3	−10.81
	3	6	3	0	5	3	15 823 620.3	−29.93
	3	6	2	0	5	2	15 823 561.6	−18.17
	3	6	1	0	5	1	15 823 539.1	0.95
	3	6	0	0	5	0	15 823 529.1	4.72
	3	6	1	0	7	1	15 650 792.8	−17.36
	3	6	0	0	7	0	15 650 782.8	−15.24
	3	6	2	0	7	2	15 650 842.5	−4.27
	3	6	3	0	7	3	15 650 889.7	−19.39
	3	6	5	0	7	5	15 651 132.7	15.37

TABLE I. (*Continued.*)

(C) 525.3 cm^{-1} band	ν'	J'	K'	ν''	J''	K''	Frequency	Observed–calculated
	3	7	6	0	6	6	15 835 592.6	2.21
	3	7	5	0	6	5	15 835 412.5	0.16
	3	7	3	0	6	3	15 835 164.9	−0.08
	3	7	2	0	6	2	15 835 086.7	−3.87
	3	7	1	0	6	1	15 835 064.8	18.29
	3	7	0	0	6	0	15 835 054.8	22.85

stants determined from the fits are shown in Table II. The observation of *c*-type bands did not allow an independent determination of the ground and excited state *C*-rotational constants, and only $\Delta C = C' - C''$ will be discussed. The results shown in Table II were obtained by keeping the ground state constants fixed at values determined in previous THz experiments.[13] To ensure that the transitions are indeed originating in the vibrational ground state, initial fits were made by floating the ground state constants. The resulting molecular constants matched the ground state constants very well, but due to the small number of transitions the excited state constants could not be fit without strong correlation. The root-mean-square deviation of the fits is ~12 MHz, which is similar to or better than the frequency accuracy of the experiment.

1. 517.2 cm^{-1} band

A total of 32 transitions were assigned to a *c*-type vibrational band of $(H_2O)_3$ centered at 517.2 cm^{-1}, as shown in Fig. 3(a). Spectral gaps only allowed observation of the $P(3)$ and $P(2)$ *P*-branch transitions. Similarly in the *R*-branches only the $R(1)$, $R(3)$, $R(4)$, and $R(6)$ transitions were observed. Additionally, transitions with $K=0$ values are affected by an unknown perturbation and could not be assigned and fit. Even with the relatively small number of observed transitions, an unambiguous assignment was possible and the results of the fit are shown in Table II.

TABLE II. The results of the fits of the 500 cm^{-1} bands are shown. The values of the ground state constants were fixed to the values determined by Brown *et al.*,[b] D_k' was fixed as it could not be fit without correlation. All values are in MHz. $\Delta\Delta = \Delta B - 2\Delta C$ is related to the difference in inertial defect, $\Delta(\Delta = I_c - I_a - I_b)$, between the excited state and ground state. Like the inertial defect, it is a measure of planarity of a molecule, with a planar molecule having $B - 2C = 0$, and $\Delta = 0$, and a negative sign indicates nonplanarity. γ is a constant introduced to take account of the $K=1$ splittings in the 523.9 cm^{-1} band. The dramatic decrease of the rotational constants is remarkable and is indicative of significant structural rearrangement. The observed value of $\Delta\Delta$ for the 525.3 cm^{-1} band shows a more planar structure in the excited state.

	Ground State[a]	517.2 cm^{-1} [a]	523.9 cm^{-1} [a]	525.3 cm^{-1} [a]
E_0	0.0(fixed)[b]	15 503 814 (6)	15 706 153 (5)	15 748 986 (4)
$B(=A)$	6646.91(fixed)[b]	6567.9 (7)	6537.8 (8)	6525.3 (4)
ΔC	0(fixed)	−29.84 (3)	−60.44 (7)	−110.64 (8)
D_J	0.0417(fixed)[b]	0.292 (12)	−0.074 (29)	0.087 (7)
D_{JK}	−0.063(fixed)[b]	−0.305 (13)	0.202 (37)	−0.111 (20)
D_K	0.027(fixed)[b]	0 (fixed)	0 (fixed)	0 (fixed)
γ			16.81 (4)	
$\Delta\Delta$		−19	+12	+100
RMS		12.88	12.55	11.94

[a] 1σ uncertainties of fitted constants in parentheses.
[b] Brown *et al.* (Ref. 13).

2. 517.5 cm^{-1} band

Although the transitions of a band centered at 517.5 cm^{-1} can be assigned to $(H_2O)_3$ via isotopic substitution experiments and the observation of combination differences for $(H_2O)_3$, they could not be definitely assigned or fit to a satisfactory degree. The transitions possibly belong to a hot band, judging by the combination differences. The appearance of the *Q*-branch is not that typically expected for an oblate symmetric top and both in the *P*- and *R*-branches a larger number of lines were observed than expected. The band appears to be split into two subbands, possibly by a Coriolis interaction, and all previously observed *a*- and *c*-type bands of $(D_2O)_3$ and $(H_2O)_3$ hot bands were split into two subbands by Coriolis interactions as illustrated in one of the preceding papers.[11,13,15] Presently we are unable to make a definitive assignment, although it is clear that spectral carrier for the 517.5 cm^{-1} band is $(H_2O)_3$.

3. 523.9 cm^{-1} band

A total of 35 transitions were assigned to a *c*-type vibrational band of $(H_2O)_3$ centered at 523.9 cm^{-1} [see Fig. 3(b)]. Spectral gaps only allowed observation of the $P(1)-P(5)$ *P*-branch transitions. Similarly only $R(3)$ was observed for the *R*-branch transitions. Although the region of the $R(5)$ transition was scanned, this laser mode appears to have severe drift and no satisfactory frequency calibration was possible. This is also shown by the fact that it was only possible to assign very few of the *Q*-branch transitions of the 525.3 cm^{-1} band, which were scanned with the same mode. The inset of Fig. 3(b) shows a comparison of the simulated (4 K rotational temperature) and observed *Q*-branch. The $Q_1(1)$ transition is split into an equal intensity doublet. This was observed for all transitions involving $K=1$. The magnitude of the splitting is *J*-dependent and could be fit well by adding a term $\pm\gamma J(J+1)$ for all $K=1$ states to the usual oblate rotational top energy expression. Although the explicit source of this splitting is unknown, it has also been observed for the degenerate vibrational levels of $(H_2O)_3$ but not for nondegenerate levels as in this case. It appears that all $K=0$ transitions are affected by a *J*-dependent perturbation similar to the $K=1$ transitions, and only $P_0(1)$ was identified. Unfortunately, extensive analysis of the entire spectral region did not allow unambiguous identification of the other

$K=0$ transitions. The results of the fit are shown in Table II. Although the quality of the fit is within the experimental uncertainty, the distortion constants for the 523.9 cm^{-1} band are unusual. In all other water trimer vibrational states observed to data, the value of D_J has been positive and the value of D_{JK} negative. Together with the perturbed $K=0,1$ transitions this leads us to the conclusion that the unusual values result from an unknown perturbation which has not been rigorously included in the fit.

4. 525.3 cm^{-1} band

A total of 62 transitions were assigned to a *c*-type vibrational band of $(H_2O)_3$ centered at 525.3 cm^{-1} [see Fig. 3(c)]. As mentioned above, the *Q*-branch region appears to have been scanned with an inferior laser mode. Even without many *Q*-branch transitions this band has the most complete set of *P*- and *R*-branch transitions and $P(1)-P(7)$ and $R(1)-R(7)$ were observed, although some of the weaker transitions within the higher *J*-value clumps were not observable. The fact that not necessarily the strongest *Q*-branch transitions were identified is puzzling and to ensure the validity of our assignments a fit with only *P*- and *R*-branch transitions was made, yielding identical results within the error of the fit. The $K=0$ and $K=1$ transitions are spaced very closely in frequency and could not be resolved as two separate transitions. This can be demonstrated by inspection of the $P(3)$ clump [see inset in Fig. 3(c)], where the low frequency line, corresponding to the convolution of the $P_0(3)$ and $P_1(3)$ transitions, clearly has a larger linewidth than the high frequency line, corresponding to the $P_2(3)$ transition. For the fit the two lines were assumed to be spaced by 10 MHz, which corresponds to the value obtained by fitting the $P(3)$ transitions as a convolution of three Gaussian line shapes. Varying this spacing did not have a significant influence on the molecular constants and the results of the fit are shown in Table II.

IV. VIBRATIONAL ASSIGNMENT

The selection rules of the G_6 symmetry group of the water trimer allow *c*-type transitions from the vibrational ground state (A_1^+) only to levels of A_1^- symmetry. There are six fundamental vibrational frequencies calculated by *ab initio* methods between 340 and 860 cm^{-1} for the asymmetric equilibrium structure of $(H_2O)_3$.[3–5] Table III shows these calculated harmonic vibrational frequencies and intensities, together with the type of motion and the symmetries of the normal modes in G_6. Only one fundamental vibrational band with the correct symmetry, the A_1^- (nondegenerate) OOP libration, is predicted to occur in the entire librational band region, in contrast to the observation of three bands originating in the ground state of the molecule. However, intensity borrowing of other librational modes needs to be considered, as Klopper *et al.*, who studied various stationary points on the torsional potential energy surface, found that a separate treatment of the different librational motions is not possible, due to coupling between all liberations.[5] Consideration of these other torsional structures also resulted in a lowering of the librational frequencies. Inspection of the nuclear displacements calculated by Xantheas *et al.* reveals that a rigorous separation into IP and OOP liberations is also misleading as all vibrations contain both IP and OOP contributions.[38] Therefore description of the observed vibration as the A_1^- OOP libration serves only as a label, and furthermore it is likely that the other librational modes borrow intensity from this OOP libration, perhaps allowing observation of *c*-type transitions for those modes. Inspection of Table III reveals that the calculated frequencies of the various librational modes differ by 130–350 cm^{-1} from the A_1^- OOP libration, in contrast to the present observation of three librational bands within 8 cm^{-1}. Overtones of lower frequency vibrational bands are expected to have lower intensity than the very intense transitions we observed here. Therefore, we conclude, taking intensity borrowing by other modes and the limitations of the harmonic approximation into account, that the observed bands do not arise from different fundamental librational modes, but rather just from one A_1^- vibrational mode, most likely the nondegenerate OOP libration. It is likely that the other librational modes have not yet been observed, as only a small part of the frequency range of ~350–830 cm^{-1} has been investigated. The observation of at least three vibrational subbands rather arises from a splitting of the rovibrational transitions by the bifurcation tunneling motion, as explained in the next section.

TABLE III. The calculated harmonic vibrational frequencies and intensities, together with the type of motion and the symmetries of the normal modes in G_6 are shown. The frequencies calculated by Klopper and Xantheas do not vary significantly.[a,b] Due to torsional averaging, the ground state wave function of the trimer is effectively that of an oblate symmetric top and so we expect a degenerate OOP and IP vibration. All frequencies are in cm^{-1} and intensities in km/mol. The only allowed parallel transition from the A_1^+ ground state is to the A_1^- OOP librational state at ~680 cm^{-1}.

Symmetry	Klopper[a]	Type of motion	Xantheas[b]	Intensity[c]
A_3^-, A_2^-	346.9	in-plane libration	346	95
	443.2		446	132
A_3^+, A_2^+	358.1	out-of-plane libration	356	37
	559.8		574	148
A_1^-	697.1	out-of-plane libration	668	291
A_1^+	827.9	in-plane libration	864	11

[a]Klopper *et al.* (Ref. 6).
[b]Xantheas (Ref. 41).
[c]Xantheas *et al.* (Ref. 3).

V. ANALYSIS AND DISCUSSION

Altogether three VRT bands of $(H_2O)_3$ have been measured previously, all of which occur at frequencies below 100 cm^{-1}.[13,39] The molecular constants of these energy levels, together with some characteristics of the observed bands, are given in Tables IV and V. Two tunneling pathways have been identified in VRT spectra of $(H_2O)_3$. The first consists of the torsional flipping motion of the free hydrogen atoms to the opposite side of the oxygen ring framework, also causing the observed vibrational averaging to an oblate symmetric top (see Fig. 1 in the preceding paper). For $(H_2O)_3$ the barrier for this motion is less than the zero-point energy of the

TABLE IV. The molecular constants for the previously observed $(H_2O)_3$ torsional transitions are shown.[b] All values are in MHz except for ζ which is dimensionless. ξ and $|\mu_{++}|$ are parameters introduced to take the Coriolis perturbations into account and $\Delta\Delta$ is defined as in Table II. The change of the rotational constants is about one order-of-magnitude smaller than for the 500 cm^{-1} bands.

(k,n)	$0^{0\,a}$	$+1^{0\,a}$	$-1^{0\,a}$	$+2^{0\,a}$	$-2^{0\,a}$	$3^{0\,a}$
E_0	0.0[b]	680 605.3 (4)		1967 970.0 (3)		2609 774.9 (2)
$B(=A)$	6646.91 (2)	6641.73 (4)		6632.11 (2)		6626.10 (2)
ΔC	0	2.37 (2)		4.09 (2)		0.79 (1)
D_J	0.0417 (2)	0.041 (1)	0.0413 (9)	0.0410 (5)	0.0404 (4)	0.0405 (3)
D_{JK}	−0.0631 (6)	−0.064 (3)	−0.064 (2)	−0.063 (2)	−0.062 (1)	−0.0627 (8)
D_K	0.027 (2)	0.030 (3)	0.028 (3)	0.028 (3)	0.027 (2)	0.027 (2)
ξ	0.0	−0.053 02 (2)		−0.039 50 (2)		0.0
$\lvert\mu_{++}\rvert$	0.0	15.344 (2)		17.47 (1)		0.0
$\Delta\Delta$	0	−9.98		−23.04		−22.45

[a]1σ uncertainties of fitted constants in parentheses.
[b]Brown *et al.* (Ref. 13).

torsional mode associated with the tunneling pathway, resulting in splittings of many wave numbers, and all previously observed $(H_2O)_3$ bands arise from transitions between these levels. These $(H_2O)_3$ bands share a very distinctive feature in that each transition is split into a (usually) equally spaced quartet with a characteristic intensity pattern, which is caused by the second tunneling motion viz. bifurcation. The bifurcation tunneling motion has been investigated in detail by Wales[2,40] and has been determined to consist of the exchange of a bound and a free hydrogen of one water molecule together with an odd number of flips of neighboring water molecules, indicative of coupling between the torsional motion (flip) and the bifurcation tunneling pathway.[39] The pathway connects eight degenerate minima on the potential energy surface, and the tunneling motion thereby splits each level into four states (A_g, T_u, T_g, A_u) with absolute nuclear spin weights of 11:9:3:1 when $K=3n$ and 8:9:3:0 when $K\neq 3n$. The magnitude of the tunneling splitting of transitions originating in the ground state is ~250–300 MHz. The observed splittings corresponds to either the difference or the sum of the tunneling splittings in the ground and excited states (see Table V). The tunneling splitting increases only slightly with torsional energy for both $(H_2O)_3$ and $(D_2O)_3$, showing that the effective barrier in the excited states is nearly identical to the ground state, and indicating only weak coupling of the torsional motion with the tunneling pathway.[41] Similarly, the degenerate hydrogen bond stretch vibration does not appear to couple strongly to the tunneling motion, as the magnitude of the tunneling splitting in the excited state is identical to that of the ground state.[16]

TABLE V. The frequencies and the magnitude of the bifurcation tunneling splitting of all previously observed $(H_2O)_3$ bands are shown.[a] The 42.9 cm^{-1} band originates from the first excited torsional state and in contrast to the other bands, the observed tunneling splitting corresponds to the difference between the ground and excited states.

Frequency (cm^{-1}) [a]	Assignment[a]	Tunneling splitting (MHz)[a]
42.9	$\pm 2^0 \leftarrow \pm 1^0$	39
65.6	$\pm 2^0 \leftarrow 0^0$	255
87.1	$\pm 3^1 \leftarrow 0^0$	289

[a]Brown *et al.* (Ref. 13).

Initially, it seemed puzzling that no such equally spaced splitting of each rovibrational transition by bifurcation tunneling was easily identifiable for the 500 cm^{-1} bands. However, the observation of at least three bands within 8 cm^{-1}, which cannot be rationalized by distinct vibrational modes, indicates that the splitting due to the bifurcation tunneling motion is dramatically increased, and the effective barrier height thereby decreased in the excited vibrational state at ~500 cm^{-1}. Wales and Fowler and Schaefer calculated bifurcation tunneling barrier heights of 381 cm^{-1} (at the DZP/MP2 level) and 523 cm^{-1} [(TZ2P+diff)/CCSD] including corrections for the zero point energy in the tunneling coordinate for $(H_2O)_3$.[2,42] If the barrier for bifurcation tunneling is indeed in this range, excitation of a 500 cm^{-1} vibrational mode will result in a dramatically reduced effective barrier height in the excited state, and consequently increased tunneling splittings, if this vibration is associated with the tunneling pathway. Inspection of Fig. 1 shows that the nuclear displacements of the water molecule exchanging the free and bound hydrogen along the beginning of the bifurcation tunneling pathway resemble an OOP librational motion. The OOP libration thus directly involves the hydrogen bond breaking motion of the rotating water monomer, and it is likely that the OOP libration is directly associated with this tunneling pathway, resulting in an increase of the tunneling splitting in the excited state of ca. three orders-of-magnitude. Therefore we propose that the bands at 517.2, 523.9, and 525.3 cm^{-1} originating from the vibrational ground state correspond to three of the four bifurcation tunneling components.

For the torsional states the individual bifurcation tunneling components are usually equally spaced with relative intensities determined by the nuclear spin weights. However, for the low barrier case proposed for the librational mode, tunneling between nonadjacent minima on the IPS may contribute considerably to the overall tunneling in the excited state, resulting in an unequal splitting.[43] Due to the unreliable relative intensities obtained in the diode laser experiment, especially over the range of many wave numbers, identification of the symmetries of the quartet tunneling components based on the relative intensities predicted by nuclear spin-weights is unreliable. Furthermore, we only expect to be able to identify three of the four tunneling com-

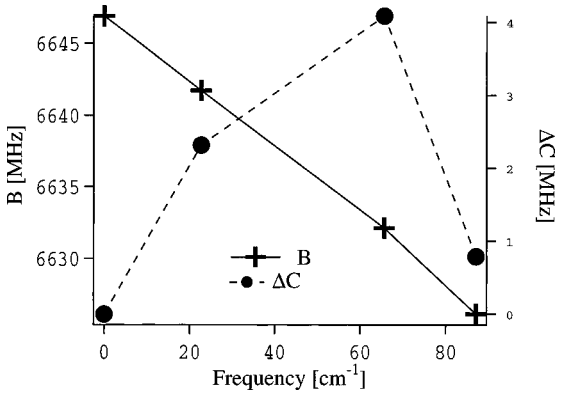

FIG. 4. The *B*-constant of all previously observed torsional states decreases nearly linearly with vibrational energy. ΔC is always positive leading to a more negative inertial defect, indicative of an out-of-plane torsional vibration.

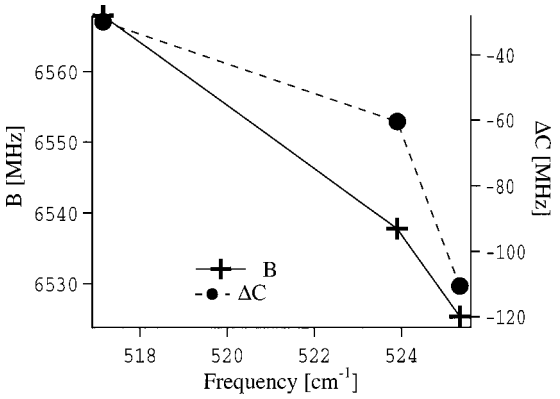

FIG. 5. Both the *B*- and *C*-rotational constants decrease dramatically in the excited states of the 500 cm^{-1} bands. Comparison with Fig. 4 reveals the change to be more than an order-of-magnitude larger than in all previously observed states. The 525.3 cm^{-1} band has a far less negative inertial defect than the other bands indicative of a torsional motion towards a more planar structure.

ponents, due to the fact that one of the *A*-states has nonzero intensities only for $K=3n$. Together with the fact that the $K=0$ levels for most bands appear to be perturbed, this will essentially preclude identification of this *A*-state with the existing data set. In addition to the incompletely characterized hot band at 517.5 cm^{-1} there is evidence for a band in close vicinity of the 523.9 and 525.3 cm^{-1} bands. Although we are confident that the three assigned subbands arise from bifurcation tunneling, we are presently unable to determine their tunneling symmetries, and cannot unambiguously determine that they belong to one quartet of states. Therefore, further work is required to confirm the assignment of these three bands to specific bifurcation tunneling components.

Further insight into the nuclear motions of a vibration can often be gained by inspection of the change of molecular constants on excitation of a vibration. For the torsional energy levels, the *B*-rotational constant decreases with increasing torsional energy, whereas the *C*-rotational constant is larger for all excited torsional energy levels than for the ground state (see Fig. 4). This leads to a more negative value of $B-2C$, and thus the inertial defect in the excited states, consistent with excitation of an out-of-plane torsional vibration. The overall change of the rotational constants relative to the ground state is smaller than 0.3% for all torsional states. However, care has to be taken in such a direct interpretation of molecular constants with respect to structural parameters as the rotational constants can be severely contaminated by perturbations and state mixing.

Given the evidence of perturbations and the possibility of state mixing, an interpretation of the molecular constants of the librational states has to be carried out with care. However, it still is interesting to attempt such interpretation. Figure 5 shows a graph of ΔB and ΔC vs. the vibrational energy for the librational bands. The changes of the rotational constants relative to the ground state (ΔB: $-1.2\%, -1.6\%, -1.8\%$; ΔC: $\sim -0.8\%, \sim -1.7\%, \sim -3.2\%$ for the 517.2, 523.9, and 525.3 cm^{-1} bands, respectively) are about one order-of-magnitude larger than those observed for any water cluster vibration, save for the dimer, and they decrease dramatically with increasing energy of the librational band. The water dimer is the only other water cluster, which shows such large changes ($\sim$1%) of the rotational constants. The reason for this is that the dimer, having just one hydrogen bond, is less rigid than all other water clusters. It has three low barrier tunneling motions, and large changes in the rotational constants are sometimes observed upon excitation of large amplitude vibrations associated with these motions. The only such facile large amplitude motion previously observed in the water trimer is the torsional motion of the free hydrogen atoms. In that case, the ground state wave function is already fully delocalized over this torsional subspace and excitation of the torsional modes therefore does not change the rotational constants significantly. If the molecular constants are not contaminated by perturbations, the very large changes of the rotational constants observed for the librational bands reported here imply significant structural differences between the vibrational ground state and the excited state, consistent with excitation of a large amplitude libration that facilitates the bifurcation tunneling motion.

The large decrease in the *B*- and *C*-rotational constants implies participation of IP librational, translational, or torsional motion. An estimate of the contribution of these motions, consistent with the observed changes in the rotational constants, can be obtained by keeping all other intermolecular coordinates fixed and only varying the average in plane (OH$\cdots$O) angles or O–O distances, respectively. A large increase of the average in plane (OH$\cdots$O) angle (between $\sim+13°$–$20°$ for the different bands) or an increase of the O–O distance of .02–.03 Å ($\sim$0.6%–1%) is required to rationalize the observed decrease in the *B*-rotational constants. Presently, we are unable to determine the sizes of contributions from IP librational and translational motions, although the strong coupling of IP and OOP librations found by Xantheas *et al.* and Klopper *et al.* indicate that most of the contribution results from IP motions.

The inertial defect becomes slightly more negative for the 517.2 cm^{-1} band, indicating a less planar structure in the excited vibrational state than in the ground state. For the pure OOP libration, such a slight increase in nonplanarity is likely, but the large decrease of the *B*-rotational constant for

this band still implies additional contributions from either translation or IP libration. In contrast, the inertial defect becomes more positive for the 523.9 cm^{-1} band and especially the 525.3 cm^{-1} band (see Table II) indicating an increased planarity in the excited state. This requires a large decrease of the torsional angles of the free hydrogens (e.g., one hydrogen in the plane). This coupling to the flipping motion shows that the nuclear displacements for these librational bands indeed resemble the bifurcation tunneling pathway very closely, since we now know that bifurcation is accompanied by a single flip.[39] Therefore, we conclude from the analysis of the rotational constants, that if they are not strongly contaminated, a new large amplitude motion has been excited and that this motion greatly facilitates the bifurcation tunneling pathway, resulting in tunneling splittings on the order of several wave numbers.

It is also interesting that the rotational constants for the individual tunneling components vary so much. The rotational constants of the 525.3 cm^{-1} band could, for example, correspond to the transition state of the bifurcation tunneling pathway. Although it seemingly contradicts the definition of a transition state that the averaged structure corresponds to a local maximum in the potential, Sabo *et al.* have shown that this is possible if the barrier is lower than the energy of the vibrational state.[44] For the torsional vibrations, the wave functions of certain states (which are analogous to the tunneling components of the bifurcation motion) have their maxima at the transition state for the tunneling motion. In the low barrier case that applies to the excited state of the 500 cm^{-1} bands, the wave functions are probably delocalized over the entire subspace of the bifurcation pathway, and correlation of rotational constants with structural parameters is not straightforward. Knowledge of the location of the nodes and maxima of the wave function with respect to the corresponding structures is necessary to fully rationalize the observed rotational constants.

The first observation of a translational vibration of $(D_2O)_3$ reported in the accompanying paper and the librational band of $(H_2O)_3$ reported here represent a major extension of the water trimer VRT data set to higher energies, and all types of intermolecular vibrations (torsion, translation, and libration) have now been observed.[16] The libration is a new large amplitude motion sampling a large part of the IPS that was not directly probed by the previously reported torsional and translational vibrations. The large data set for the water trimer will allow rigorous tests of existing potentials. Analysis of the librational band indicates extensive coupling between the librations, torsions, and most likely translations. Therefore calculations including all 12 intermolecular degrees of freedom are probably necessary to reproduce the experimental data. Inclusion of this extensive data set into a fit of existing potentials is the next step in determination of an accurate water potential, as the water trimer allows explicit quantification of the three-body forces.

The results presented here should also aid in the exact determination of the barrier height for the bifurcation tunneling pathway in the water trimer. Again, bifurcation is the lowest energy process in water clusters that effects the breaking and reforming of hydrogen bonds. It is interesting that excitation of a libration results in a dramatically increased bifurcation tunneling splitting, as librations are the dominant motion for breaking of hydrogen bonds in the bulk, and thus are of special significance in liquid water. An investigation of the detailed effects of exciting the various intermolecular vibrations of the water trimer on the bifurcation tunneling splitting is ongoing.[43]

VI. CONCLUSIONS

We have presented diode laser VRT results characterizing four *c*-type librational bands between 515 and 528 cm^{-1}, extending high-resolution VRT data to much higher energies than previously available. We assign the vibrations to the nondegenerate A_1^- OOP libration, although extensive coupling with IP librations and torsional motions is evident. The large observed change in rotational constants is rationalized by ''activation'' of a new large amplitude motion. Together with the observation of at least three bands within 8 cm^{-1} this is indicative of that the vibration is facilitating the bifurcation tunneling, resulting in dramatically increased tunneling splittings. This should allow an exact determination of the barrier height for this important tunneling pathway.

Further theoretical calculations at a higher level than currently available are necessary to extract a detailed understanding of the energy levels in this frequency region, which are probably immersed in a high density of background states. In conjunction with this, further experimental efforts are clearly necessary to investigate this spectral region in more detail.

ACKNOWLEDGMENTS

The authors wish to thank Dr. Alenka Luzar for helpful discussion regarding bulk dynamics and Dr. Sotiris Xantheas for the nuclear displacements of the librational vibrations. This work was supported by the Experimental Physical Chemistry Program of the National Science Foundation.

[1] S. Suzuki and G. A. Blake, Chem. Phys. Lett. **229**, 499 (1994).
[2] D. J. Wales, J. Am. Chem. Soc. **115**, 11180 (1993).
[3] S. S. Xantheas and T. H. Dunning, Jr., J. Chem. Phys. **99**, 8774 (1993).
[4] S. S. Xantheas and T. H. Dunning, J. Chem. Phys. **98**, 8037 (1993).
[5] W. Klopper, M. Schütz, H. P. Lüthi, and S. Leutwyler, J. Chem. Phys. **103**, 1085 (1995).
[6] W. Klopper and M. Schütz, Chem. Phys. Lett. **237**, 536 (1995).
[7] K. Liu, M. G. Brown, C. Carter, R. J. Saykally, J. K. Gregory, and D. C. Clary, Nature (London) **381**, 501 (1996).
[8] K. Liu, J. D. Cruzan, and R. J. Saykally, Science **271**, 929 (1996).
[9] K. Liu, M. G. Brown, J. D. Cruzan, and R. J. Saykally, Science **271**, 62 (1996).
[10] R. S. Fellers, C. Leforestier, L. B. Braly, and M. G. Brown, Science **284**, 945 (1999).
[11] M. R. Viant, M. G. Brown, J. D. Cruzan, R. J. Saykally, M. Geleijns, and A. van der Avoird, J. Chem. Phys. **110**, 4369 (1999).
[12] M. G. Brown, F. N. Keutsch, and R. J. Saykally, J. Chem. Phys. **109**, 9645 (1998).
[13] M. G. Brown, M. R. Viant, R. P. McLaughlin, C. J. Keoshian, E. Michael, J. D. Cruzan, R. J. Saykally, M. Geleijns, and A. van der Avoird, J. Chem. Phys. **111**, 7789 (1999).
[14] M. G. Brown, F. N. Keutsch, L. B. Braly, and R. J. Saykally, J. Chem. Phys. **111**, 7801 (1999).
[15] F. N. Keutsch, E. N. Karyakin, R. J. Saykally, and A. van der Avoird, J. Chem. Phys. **114**, 3988 (2001), this issue.
[16] F. N. Keutsch, P. B. Petersen, M. G. Brown, R. J. Saykally, M. Geleijns,

and A. van der Avoird, J. Chem. Phys. **114**, 3994 (2001), preceding paper.
[17] T. Dyke and J. Muenter, J. Chem. Phys. **60**, 2929 (1973).
[18] K. L. Busarow, R. C. Cohen, G. A. Blake, K. B. Laughlin, Y. T. Lee, and R. J. Saykally, J. Chem. Phys. **90**, 3937 (1989).
[19] J. D. Cruzan, L. B. Braly, K. Liu, M. G. Brown, J. G. Loeser, and R. J. Saykally, Science **271**, 59 (1996).
[20] J. D. Cruzan, M. G. Viant, M. G. Brown, D. D. Lucas, L. Kun, and R. J. Saykally, Chem. Phys. Lett. **292**, 667 (1998).
[21] G. C. Groenenboom, E. M. Mas, R. Bukowski, K. Szalewicz, P. E. S. Wormer, and A. van der Avoird, Phys. Rev. Lett. **84**, 4072 (2000).
[22] Y.-L. Yeh and C.-Y. Mou, J. Phys. Chem. B **103**, 3699 (1999).
[23] M. J. Lang, X. J. Jordanides, X. Song, and G. R. Fleming, J. Chem. Phys. **110**, 5884 (1999).
[24] J. Teixeira, M.-C. Bellissent-Funel, and S.-H. Chen, J. Phys.: Condens. Matter **2**, SA105 (1990).
[25] S.-H. Chen, P. Gallo, F. Sciortino, and P. Tartaglia, Phys. Rev. E **56**, 4231 (1997).
[26] K. Okada, M. Yao, Y. Hiejima, H. Kohno, and Y. Kajihara, J. Chem. Phys. **110**, 3026 (1999).
[27] J. Barthel, K. Bachhuber, R. Buchner, and H. Hetzenauer, Chem. Phys. Lett. **165**, 369 (1990).
[28] I. Savatinova and E. Anachkova, Phys. Status Solidi B **91**, 413 (1979).
[29] S. Sastry, H. E. Stanley, and F. Sciortino, J. Chem. Phys. **100**, 5361 (1994).
[30] M. A. Ricci, G. Signorelli, and V. Mazzacurati, J. Phys.: Condens. Matter **2**, SA183 (1990).
[31] D. A. Draegert and D. Williams, J. Chem. Phys. **48**, 401 (1968).
[32] A. Luzar and D. Chandler, Phys. Rev. Lett. **76**, 928 (1996).
[33] A. Luzar (private communication).
[34] A. Luzar and D. Chandler, J. Chem. Phys. **98**, 8160 (1993).
[35] L. M. Goss, S. W. Sharpe, T. A. Blake, V. Vaida, and J. W. Brault, J. Phys. Chem. A **103**, 8620 (1999).
[36] A. Van Orden, T. F. Giesen, R. A. Provencal, H. J. Hwang, and R. J. Saykally, J. Chem. Phys. **101**, 10237 (1994).
[37] M. R. Viant, R. S. Fellers, R. P. McLaughlin, and R. J. Saykally, J. Chem. Phys. **103**, 9502 (1995).
[38] Xantheas (private communication).
[39] E. H. T. Olthof, A. van der Avoird, P. E. S. Wormer, K. Liu, and R. J. Saykally, J. Chem. Phys. **105**, 8051 (1996).
[40] D. J. Wales, J. Chem. Soc., Faraday Trans. **92**, 2505 (1996).
[41] M. G. Brown, Ph.D. thesis, University of California Berkeley, 1999.
[42] J. E. Fowler and H. F. Schaefer, J. Am. Chem. Soc. **117**, 446 (1995).
[43] F. N. Keutsch, R. S. Fellers, M. G. Brown, M. R. Viant, P. B. Petersen, and R. J. Saykally, J. Am. Chem. Soc. (in press).
[44] D. Sabo, Z. Bacic, S. Graf, and S. Leutwyler, J. Chem. Phys. **111**, 5331 (1999).